Journal of Chemical Health Risks

www.jchr.org

JCHR (2026) 16(1), 1402-1419 | ISSN:2251-6727

Formulation of Glatiramer Acetate Atrigel® Using DMSO as Solvent for Multiple Sclerosis Treatment

Sushant Ishwar Pote[1] Om Sambhaji Shelke[2]*, Rajesh Khathuriya[1], Vrushali A Kulkarni[4]

[1]Department of Pharmaceutics, Pacific Academy of Higher Education and Research University, Udaipur, Rajasthan, India

[2]Post Doctoral Research Scholar, Department of Pharmaceutics, Manipur International University, Imphal, Manipur, India-795140

[3]Sinomune Pharmaceutical Co., Ltd, Wuxi, Jiangsu, China-214194

[4] Amepurva Forum's Nirant Institute of Pharmacy, Boramani Solapur, Maharashtra, India

***Corresponding Author:**

Dr Om Sambhaji Shelke

Address: Post-Doctoral Research Scholar, Department of Pharmaceutics, Manipur International University, Imphal, Manipur, India-795140

(Received: 05 November 2025 Revised: 15 December 2025 Accepted: 23 January 2026)

KEYWORDS

Multiple sclerosis, Atrigel®, Depot injection, Glatiramer Acetate, PLGA, Dimethyl Sulfoxide.

ABSTRACT:

Objective: This study focused on the development and evaluation of a long-acting poly(lactic-co-glycolic acid) (PLGA)-based Atrigel® (AG) delivery system for Glatiramer Acetate (GA) to enhance therapeutic efficacy in the management of multiple sclerosis. The formulation was systematically optimised to generate a sustained-release depot upon parenteral administration, thereby mitigating the limitations associated with frequent dosing inherent to current treatment regimens.

Methods: A 3^2 randomised complete factorial design was employed to optimise critical formulation parameters such as drug-to-polymer ratio and solvent concentration. The AG system was formulated using Dimethyl Sulfoxide (DMSO) and PLGA polymer. The developed formulations were characterised for syringeability, viscosity, and in vitro drug release. Physicochemical properties were assessed, and biological evaluations included ex vivo release studies and cytotoxicity assays using the hen drumstick model and L929 fibroblasts, respectively.

Results: The optimised formulation achieved sustained drug release with reduced dosing frequency. Statistical analysis confirmed significant effects of drug-to-polymer ratio and solvent concentration on release kinetics ($p < 0.05$). An amorphous GA dispersion was formed within poly(lactic-co-glycolic acid), demonstrating good physical compatibility. Ex vivo studies demonstrated consistent release profiles ($p > 0.05$ compared with in vitro), and cytotoxicity assays indicated high biocompatibility.

Conclusion: The AG system represents a promising long-acting alternative to conventional GA therapy, providing controlled release, improved formulation stability, and the potential to enhance patient adherence. Further investigations are warranted to elucidate in vivo pharmacokinetics and to assess the scalability of this approach.

INTRODUCTION

Multiple Sclerosis (MS) is a chronic autoimmune neurological disorder that is non-traumatic, disabling, and influenced by both genetic and environmental factors. It ranks as one of the leading causes of neurological impairment among young adults [1–3]. The worldwide prevalence of MS is rising, affecting both developed and developing countries, with women being more than twice as likely to develop the condition compared to men [4, 5]. MS mainly affects young adults and presents in four clinical forms: Relapsing-remitting

Journal of Chemical Health Risks

www.jchr.org

JCHR (2026) 16(1), 1402-1419 | ISSN:2251-6727

MS (RRMS), secondary-progressive MS, primary-progressive MS, and progressive-relapsing MS. Approximately 85% of patients initially present with RRMS, characterised by episodic neurological symptoms that may partially or fully recover within days to weeks [6, 7]. MS often begins with episodes of reversible neurological deficits. Early axonal damage is crucial to disease progression and long-term disability [8, 9]. Diagnosis involves detecting inflammatory and demyelinating damage in the Central Nervous System (CNS) over various regions and time. Tests like cerebrospinal fluid analysis, evoked potentials, bladder urodynamics, and optical coherence tomography can aid diagnosis but are often unnecessary [10-12]. Several Disease-Modifying Treatments (DMTs) are now available to manage RRMS, primarily to reduce relapse rates and the severity of CNS inflammation [13]. Currently, there is no cure for MS. Recent advances have led to the development of newer, more effective treatments beyond traditional DMTs, such as Interferon Beta (IFNβ) and GA. For instance, fingolimod, the first oral DMT, received approval in the United States in 2010 [14-16]. GA not only affects neurons but also reduces demyelination and promotes myelin repair [17].

GA is a mixture of diverse polypeptides with immunomodulatory properties, approved in the U.S. in 1996 as COPAXONE and in Europe in 2001 [18, 19]. It comprises a complex mixture of polypeptides derived from four amino acids that resemble Myelin Basic Protein (MBP). These are generated by polymerising L-glutamic acid, L-alanine, L-lysine, and L-tyrosine, followed by partial hydrolysis [20, 21].

AG employs a biodegradable polymer solution that forms a solid or semi-solid depot upon injection and interacts with bodily fluids. This facilitates controlled, sustained release of therapeutic agents. Its benefits include reducing the number of doses, enhancing patient compliance, increasing drug stability, and enabling localised delivery that minimises systemic side effects. AG is used across various medical areas, such as pain management (e.g., extended-release bupivacaine), hormone therapy (e.g., leuprolide acetate for prostate cancer), and post-surgical recovery, where prolonged drug release is essential. Its ability to deliver both small molecules and biologics accurately makes it preferable to traditional bolus injections, which often cause rapid drug clearance and plasma level fluctuations. Overall, the versatility and efficiency of AG make it a promising option for long-term therapeutic delivery [22-23].

GA is used to treat MS, including clinically isolated syndrome, relapsing-remitting MS, and active secondary progressive MS in adults. It is administered as a 20 mg/mL daily injection or a 40 mg/mL three-times-weekly subcutaneous injection [22]. Although daily GA injections are standard care, patient adherence is often challenging. This study explores a long-acting AG formulation to address these issues. MS requires lifelong treatment, which complicates adherence. Despite the availability of several approved disease-modifying therapies, there remains a critical need to improve patient outcomes by enhancing treatment effectiveness, tolerability, and adherence [23,24].

In this study, a stable, efficacious, long-acting, in situ-forming GA implant of an AG-containing polymer and solvent was evaluated to improve treatment efficacy.

MATERIALS AND METHODS

Materials

GA was obtained from Pharmaffiliates in Haryana, India. Evonik India provided Resomer 202H (75:25) and other PLGA grades. Resomer 202H (75:25) was selected for its established biocompatibility and predictable degradation, making it suitable for sustained release formulations. DMSO, Ethyl Acetate (EA), N-methyl-2-pyrrolidone (NMP), and Dichloromethane (DCM) were purchased from Sigma-Aldrich, and Mannitol from DFE Pharma. Analytical chemicals from Merck Mumbai and other reputable suppliers were used as received. Penicillin-streptomycin, fetal bovine serum (FBS), RPMI 1640 culture medium, and trypsin were acquired from Gibco (Germany). The Mouse L929 fibroblast cell line was supplied by the National Centre for Cell Science.

Preparation of AG

To prepare AG, 2.5 grams of Resomer 202H was accurately weighed and placed into a vial, followed by the addition of 7.5 grams of DMSO. The vial was sealed with a rubber stopper and a flip-off seal. The polymer was then allowed to dissolve fully in the solvent. Once dissolution was complete, the mixture was checked for clarity and hydration. Before administration, the polymer phase was combined with GA powder. After thorough

Journal of Chemical Health Risks

www.jchr.org

JCHR (2026) 16(1), 1402-1419 | ISSN:2251-6727

mixing, the in situ-forming implant was prepared and ready for use [25,26].

Formulation Optimization

In the initial experiments, PLGA polymers with both acid and ester end groups, such as PLGA 50:50, PLGA 75:25, and PLGA 85:15, were utilised. Organic solvents, including DMSO, EA, NMP, and DCM, were incorporated into the formulations. Preliminary investigations assessed how key formulation and process parameters- such as drug-to-polymer ratio and solvent concentration- affect critical response variables like syringeability, evaluated through break-loose force (BLF) and glide forces (GLF), viscosity, and drug-release kinetics. To systematically optimise these factors, a 2^3 randomised complete factorial design with one centre point was employed, examining two independent variables: drug-to-polymer ratio (X_1) and solvent concentration (X_2), each at three levels (low, medium, high) within predefined ranges. All dependent variables were meticulously analysed to understand how these formulation parameters influence system performance [27, 28].

Table 1 displays the independent variables and their levels. A total of nine experimental runs, including one centre point, were conducted and systematically assessed with respect to the Critical Quality Attributes (CQAs): GLF (Y_1), viscosity (Y_2), and in vitro drug release at 90 minutes (Y_3). Optimisation processes and data analysis, including the creation of response surface plots, were performed using Design Expert® software (Version 13.0.5.0, State-Ease Inc., Minneapolis, MN).

Table 1: 3^2 Randomised full factorial Design parameters and experimental conditions

Independent variables		**X_1: Drug to Polymer ratio (mg)**	**X_2: Solvent Concentration (mg)**
Levels	**Low (-1)**	20:20	115
	Medium (0)	20:100	230
	High (+1)	20:200	345
Dependent Variables		Y_1: GLF (N) Y_2: Viscosity (Cp) Y_3: In vitro release (%)	

The experimentally observed response values were quantitatively compared with the expected research values to confirm the experimental design. The relative error (%) was determined using the following equation:

$$Relative\ Error\ (\%) = \frac{[Predicted\ Value - Experimental\ Value]}{Predicted\ value} X\ 100$$

Characterisation of AG

UV Spectroscopy

The ultraviolet absorption spectrum of drug GA was recorded in phosphate buffer at pH 7.4 over 200-400 nm using a quartz cuvette (1 cm path length) and a Shimadzu UV-1700 spectrophotometer. The peak absorption wavelength was identified for future quantitative analysis. Standard GA solutions at known concentrations were then prepared, and their absorbance was measured at this characteristic wavelength. A calibration curve was created by plotting concentration against absorbance, revealing a linear relationship that served as the basis for determining the sample content [30].

Fourier Transform Infrared Spectroscopy (FTIR)

The drug's chemical structure was examined with an attenuated total reflection FTIR/ATR spectrometer (Bruker II Alpha). The sample was maintained at approximately 25.0 ± 0.5 °C. A small amount of sample was applied to the Zinc solenoid crystal plate, and the Anvil was rotated to secure it. Spectra were obtained by scanning in the 4000-400 cm^{-1} range, and identification of different functional groups and chemical bond

Journal of Chemical Health Risks

www.jchr.org

JCHR (2026) 16(1), 1402-1419 | ISSN:2251-6727

information within the molecules was achieved through the analysis of characteristic absorption peaks [31].

Differential Scanning Calorimetry (DSC)

A DSC 250 system was used to capture thermograms of bulk GA, mannitol, Resomer 202H, the physical mixture, and the GA implant. Each sample was carefully weighed and placed into an aluminium pan with a puncture lid, using 2.0 mg of material. The analysis was performed at a nitrogen gas flow rate of 50 ml/min and a heating rate of 10 °C/min, increasing from 40 to 250 °C [31].

X-ray diffraction Pattern (XRD)

XRD patterns were recorded for GA, Polymer, and the final formulation to evaluate their physical attributes. A Rigaku Smart Lab Powder X-ray diffractometer was used to record these patterns at a scanning rate of 1 ° min-1 within the 10 °- 50 ° 2θ range [32].

Particle Morphology

The morphology of the prepared formulations was examined using scanning electron microscopy (SEM). Briefly, dry powdered particles were mounted on aluminium tubs with carbon tape and coated with gold via sputtering in an argon atmosphere under high vacuum. The samples were then examined using SEM (Hitachi SU-3500) [29].

Apparent Viscosity

The apparent viscosity of the formed depot formulation was measured using a Brookfield viscometer (Model: DV2T). An accurately measured 20 mL formulation was charged into the sample holder. The liquid-state solution was determined using an adapter: spindle T-bar T-A; spindle speed, rpm: 20; time, 10 minutes; temperature, 25 °C; and multi-average reading. The depot viscosity was determined using an adapter (spindle T-bar T-F, S-96), a spindle speed of 10 rpm, a 10-minute time, a temperature of 37°C, and an endpoint reading. The readings were noted after finishing the run [33].

Drug Loading Analysis

Sample Preparation: Weigh out exactly 5 mL of the formulation containing 100 mg of GA and transfer it into a 100 mL volumetric flask. Dissolve the sample thoroughly and dilute to the mark with purified water. Chromatographic Analysis: Inject 50 µL of the blank, standard, and sample solutions into the chromatograph, ensuring that each solution is filtered through a 0.45 µm membrane filter before injection. Quantification: Determine the average peak area from five replicate injections of the drug. Use the regression equation derived from the pure reference standard [34] to calculate the amount of the drug in the tablets.

pH Measurement

The pH of the AG formulation was measured with a pH meter (Orion Lab Star PH111). The meter was calibrated at different pH levels before dispensing the AG into the cuvette. The probe was immersed in the formulation until the reading stabilised, after which the pH was recorded [35, 36].

Study of In Vitro Dissolution

The dissolution of bulk GA powder, Physical Mixture (PM), and GA AG was tested using the USP Apparatus 2 (Distek Inc., USA, North Brunswick) with Japanese sinkers. The paddle was set to a constant 50 rpm, and the temperature was maintained at 37 ±0.5°C throughout the experiment [26].

Ex Vivo Release Study of GA AG Samples

An ex vivo release study was performed to assess the intramuscular delivery of the AG formulation, following established methodology [27]. The optimised formulation was injected subcutaneously into a hen drumstick muscle with a 20-gauge needle. The drumstick was then immersed in a beaker containing 250 ml of pH 7.4 phosphate-buffered saline with 0.1% w/v sodium azide as an antibacterial agent, maintained at 37°C throughout. The use of 0.1% w/v sodium azide, recommended by the USFDA, is standard in IVPT studies to prevent microbial growth. At set intervals (2, 6, 8, 10, 12, 18, 24, 48, and 72 hours), 3 ml of the release medium was sampled and replaced with an equal volume of fresh medium to sustain sink conditions. To confirm the formation of the AG or implant, the injection site was incised 24 hours after injection. The drug concentration in the medium was analysed via high-performance liquid chromatography (HPLC), and the cumulative release profile was calculated from these data [28].

In Vitro Cytotoxicity Assessment of Formulations on L929 Fibroblasts

The L929 fibroblast cell line, derived from mouse tissue, was cultivated in RPMI 1640 medium supplemented

Journal of Chemical Health Risks

www.jchr.org

JCHR (2026) 16(1), 1402-1419 | ISSN:2251-6727

with 10% heat-inactivated fetal bovine serum, 100 IU/mL penicillin, and 100 µg/mL streptomycin. Cells were kept at 37°C in a humidified atmosphere with 5% CO2. They were seeded in 12-well plates at a density of 5×10^4 cells per well and allowed to adhere for 24 hours. Sterilised AG, implant formulations, Dimethyl Sulfoxide, and polymer (10 µL per sample) were directly applied to the monolayer. The plates were then incubated for an additional 24 hours. Untreated cells in growth medium served as the negative control. Cell viability was assessed using the MTT assay: culture medium was removed and replaced with 500 µL of MTT solution (0.5 mg/mL in PBS). After 4 hours, the MTT solution was discarded, and the resulting formazan crystals were dissolved in 100 µL of DMSO; the plates were shaken for 1 hour. Absorbance was measured at 570 nm with a 630 nm reference wavelength using a Tecan Group Ltd. microplate reader. All experiments were done in triplicate, and data are shown as mean ± standard deviation [29, 30].

RESULTS

Formulation Optimization

Initially, DMSO, ethyl acetate, and DCM were evaluated but were discarded due to concerns about DMSO's toxicity and drug stability, ethyl acetate's high volatility, which could lead to uncontrolled release, and DCM's carcinogenic potential and regulatory challenges. NMP was selected for its moderate volatility, improved biocompatibility, and demonstrated success in FDA-approved depot formulations, thereby offering safer, more controlled drug delivery within the AG system.

Table 2: Drug Loading and BLF

Batch No:	% Drug Loading	BLF (N)	pH
AG-1	99.5 ± 0.12	10.864 ± 0.55	6.43 ± 0.05
AG-2	99.1 ± 0.15	9.612 ± 0.43	7.69 ± 0.06
AG-3	99.7 ± 0.21	7.153 ± 0.34	7.06 ± 0.02
AG-4	99.4 ± 0.05	6.956 ± 0.35	7.19 ± 0.04
AG-5	99.9 ± 0.14	5.236 ± 0.49	7.68 ± 0.07
AG-6	99.6 ± 0.18	9.252 ± 0.63	6.76 ± 0.02
AG-7	99.2 ± 0.22	5.644 ± 0.31	7.19 ± 0.05
AG-8	99.8 ± 0.07	12.106 ± 0.98	7.13 ± 0.02
AG-9	99.7 ± 0.12	14.261 ± 1.12	7.51 ± 0.04
AG-10	99.4 ± 0.23	6.994 ± 0.24	7.36 ± 0.05

n=3.

Based on the data, the GA-AG formulations demonstrated highly consistent drug loading, with percentages ranging from 99.1% to 99.9% across all batches. However, their physical properties varied considerably depending on formulation factors. The BLF, which measures the force required to expel the gel from the syringe, showed the most significant variation, ranging from 5.044 N to 14.261 N. Formulations with a higher drug-to-polymer ratio of 20:200 consistently exhibited a much higher average BLF of 14.261 N compared to the lower ratio of 20:20, which had an average BLF of 5.236 N. The pH values were generally neutral to slightly basic, spanning from 6.43 to 7.69. Overall, the drug-to-polymer ratio had a more significant impact on the gel's physical properties than solvent concentration. Both the drug-polymer ratio and solvent concentration are key factors in AG formulations, affecting system stability and drug-release behaviour.

Journal of Chemical Health Risks

www.jchr.org

JCHR (2026) 16(1), 1402-1419 | ISSN:2251-6727

These two variables notably influenced the GA-AG formulation. Consequently, a 32-run randomised complete factorial design with one replicate was employed to assess critical parameters for optimisation: solvent concentration and drug-to-polymer ratio. This study comprised nine experimental runs plus one replicate. Table 3 summarises the results for all measured responses, including GLF, viscosity, and in vitro release.

Various formulation batches of AG GA were prepared using a factorial design. The independent variables were drug-to-polymer ratio (X1) and Solvent concentration (X2).

Table 3: 3^2 Full factorial Design and response values of GA formulation.

Batch No:	Factor 1 A:Drug: Polymer (mg)	Factor 2 B: Solvent Conc (mg)	Response 1 GLF N	Response 2 Viscosity Cp	Response 3 % Release %
GA-1	20:200	230	6.657	132000	62.38
GA-2	20:100	230	5.287	129000	96.73
GA-3	20:100	345	4.348	79000	99.15
GA-4	20:20	115	4.012	108500	92.13
GA-5	20:20	345	3.109	74533	98.30
GA-6	20:20	345	3.105	74521	98.21
GA-7	20:20	230	3.764	124000	97.23
GA-8	20:200	345	4.961	103500	97.42
GA-9	20:200	115	7.215	102500	62.37
GA-10	20:100	115	4.569	144000	64.65

n=3.

ANOVA was employed to assess the relative importance of variables and to select the model for response analysis, as shown in

Table *4*. The independent variables X1 and X2 were denoted A and B, respectively, in the model. The independent factors, Drug-polymer ratio (A) and Content of solvent per unit dose, were found to be significant for GLF, Viscosity, and Drug release. A quadratic model best described the link between them.

$$GLF = + 4.88-1.25 * X_1 - 0.1453 * X_1 + 0.3853 * X_2 + 0.3560 *X_2 -0.0010*X_1X_2 -0.5510* X_1X_2-0.2197* X_1X_2+0.1963* X_1X_2……..(1)$$

$$Viscosity = + 1.108E+05 – 8438.44 * X_1+6552.56 * X_1+7552.56 * X_2+17552.56 * X_2- 1394.89 * X_1* X_2 + 19114.11* X_1* X_2 + 4105.11 * X_1* X_2 - 5885.89 * X_1* X_2 ……..(2)$$

$$\% Release = +10857.21 -10761.34* X_1 – 10770.37 * X_1 – 10784.16 * X_2 –10771.76* X_2 + 10780.42 * (X_1)* X_2 +10761.97* (X_1)* X_2 + 10773.12 * (X_1)* X_2 + 10781.65* (X_1)* X_2……..(3)$$

A positive sign shows that a factor enhances the response, while a negative sign indicates an inverse relationship between the factor and the response. Equation 2 for viscosity includes a negative coefficient for solvent concentration, suggesting that increasing solvent concentration generally reduces viscosity. The 3D response surface plot shown in the figure illustrates how a factor influences the response and elucidates the interaction between components A and B. To analyse how different parameters impacted the CQAs, the 3D

Journal of Chemical Health Risks
www.jchr.org
JCHR (2026) 16(1), 1402-1419 | ISSN:2251-6727

surface plot was used. Figure 2 displays the effects of interactions among various formulations and composition parameters on GLF, Viscosity, and % drug release.

Table 4: Analysis of variance (ANOVA) statistical Model

Source	GLF (Y1)					Viscosity (Y2)					% Release (Y3)				
	Sum of Squares	df	Mean Square	F-Value	P-Value	Sum of Squares	df	Mean Square	F-Value	P-Value	Sum of Squares	df	Mean Square	F-Value	p-Value
Model	17.13	8	2.14	2.677 E+05	0.0015	5.694 E+09	8	7.118 E+08	9.886 E+06	0.002	8.460 E+09	8	1.058 E+09	2.611 E+11	< 0.0001
A-Drug : Polymer	11.40	2	5.70	7.122 E+05	0.008	4.416 E+08	2	2.208 E+08	3.067 E+06	0.004	2.571 E+09	2	1.285 E+09	3.174 E+11	< 0.0001
B-Solvent Conc	2.65	2	1.32	1.654 E+05	0.017	3.562 E+09	2	1.781 E+09	2.473 E+07	0.001	1.792 E+09	2	8.962 E+08	2.213 E+11	< 0.0001
AB	1.23	4	2.14	38513 .89	0.038	1.177 E+09	4	2.943 E+08	4.087 E+06	0.004	4.478 E+09	4	1.119 E+09	2.764 E+11	< 0.0001
Residual	-	-	-	-	-	-	-	-	-	-	-	-	-	-	-
Lack of Fit	-	-	-	-	-	-	-	-	-	-	-	-	-	-	-
Pure Error	8.000E-06	1	8.000E-06	-	-	72.00	1	72.00	-	-	0.0041	1	0.0041	-	-
Cor Total	17.13	9	-	-	-	5.695 E+09	9	-	-	-	8.460 E+09	9		-	-

Note: df-degree of freedom.

Journal of Chemical Health Risks

www.jchr.org

JCHR (2026) 16(1), 1402-1419 | ISSN:2251-6727

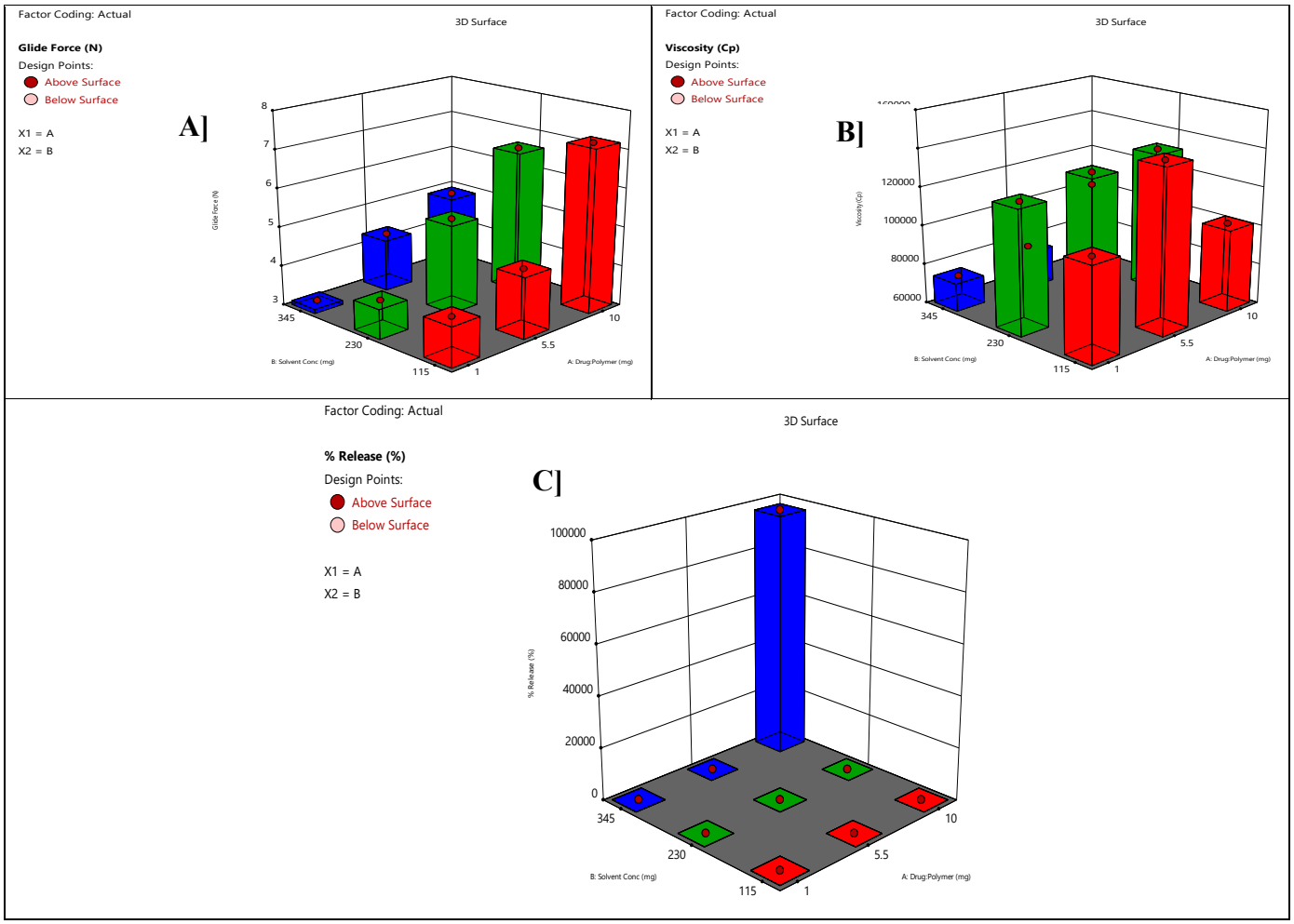

Figure 1: 3D response surface plot representing the interpretation of independent variables on A] GLF, B] Viscosity, C] % Release.

The accuracy of the optimised formula was confirmed by comparing observed values with predicted responses. The experimental results fell within the expected range, as shown in Table 5. The relative error between expected and observed results was less than 5%. To improve the AG depot formulations, a 23-way randomised complete factorial design was validated.

Table 5: Optimised formulation compositions and predicted vs. observed response values.

Optimized Formulation	Optimized concentration	Responses	Predicted Value	Observed value	% Relative Error
Drug: Polymer Ratio	20:200	GLF	7.215	7.305	1.242
Content of solvent per unit dose	115	Viscosity	102500	102637	0.064
		% Release	62.370	61.18	-2.162

Journal of Chemical Health Risks

www.jchr.org

JCHR (2026) 16(1), 1402-1419 | ISSN:2251-6727

Characterisation of AG

UV calibration curve of GA

The ultraviolet-visible analysis of GA in PBS (pH 7.4) revealed a λmax at 275 nm, consistent with the chromophoric properties of GA's polypeptide structure, as shown in **Figure 2**B. The calibration curve has demonstrated excellent linearity (R^2 = 0.998) when constructed by plotting absorbance versus GA concentration (range: 0-80 µg/mL). The curve exhibited confirming adherence to the Beer-Lambert law, as shown in **Figure 2** A]. This validated linear relationship demonstrates the method's suitability for accurate quantification of GA in dissolution testing and in vitro release studies.

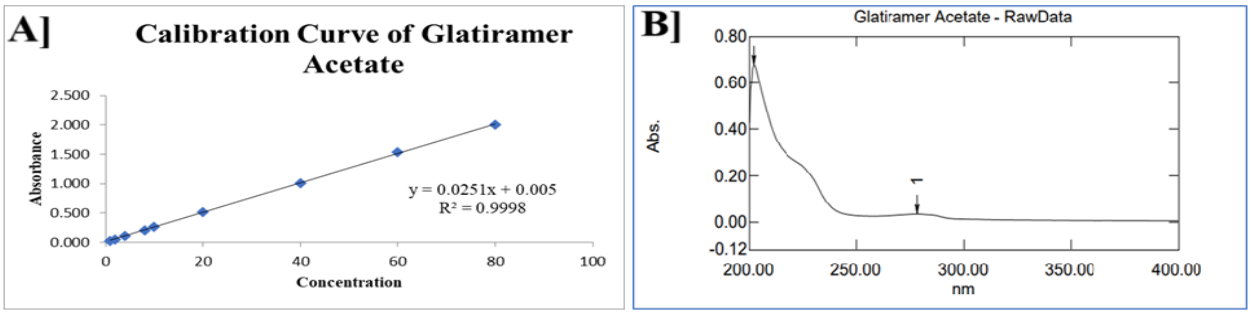

Figure 2: A] UV Calibration curve; B] **λmax of GA**

Fourier Transform Infrared Spectroscopy (FTIR)

Spectral analysis of the physical mixture demonstrated characteristic absorption bands corresponding to both components: the amide I (~1650 cm^{-1}), amide II (~1540 cm^{-1}), and carboxylic group (~3298 cm^{-1}) vibrations of GA's peptide backbone, along with the ester carbonyl stretch (~1750 cm^{-1}) of PLGA. The results demonstrate that the molecular integrity of GA is preserved, with no significant chemical interactions observed during formulation processing, as shown in **Figure *3***. The FTIR spectra revealed characteristic peaks of GA (amide I at ~1650 cm^{-1}) and PLGA (ester C=O at ~1750 cm^{-1}). Although these peaks overlap, no new absorption bands were observed, confirming the absence of covalent interactions between GA and PLGA and indicating chemical stability in the formulation. This suggests that the drug-polymer interaction is primarily physical, supporting the integrity of the AG system.

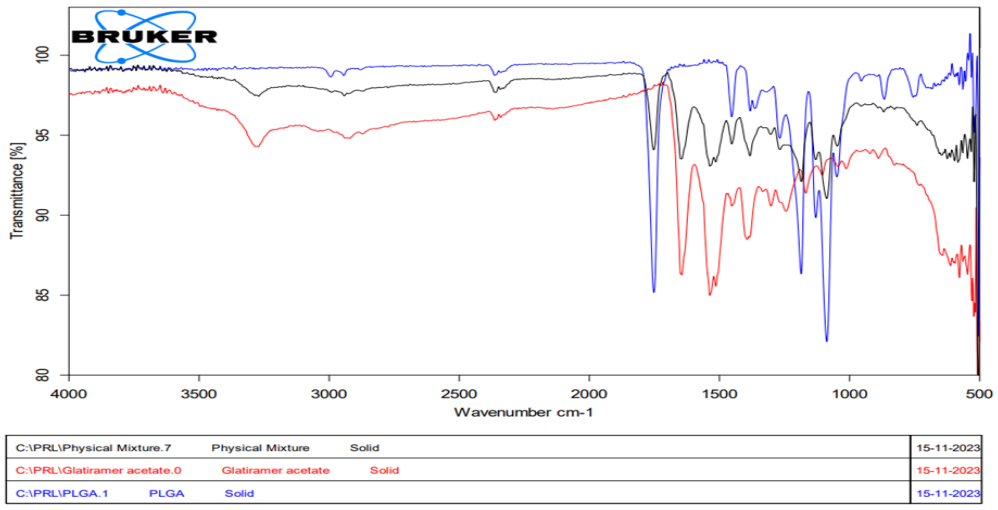

Journal of Chemical Health Risks

www.jchr.org

JCHR (2026) 16(1), 1402-1419 | ISSN:2251-6727

Figure 3: FTIR Spectra of GA, Physical Mixture & Polymer.

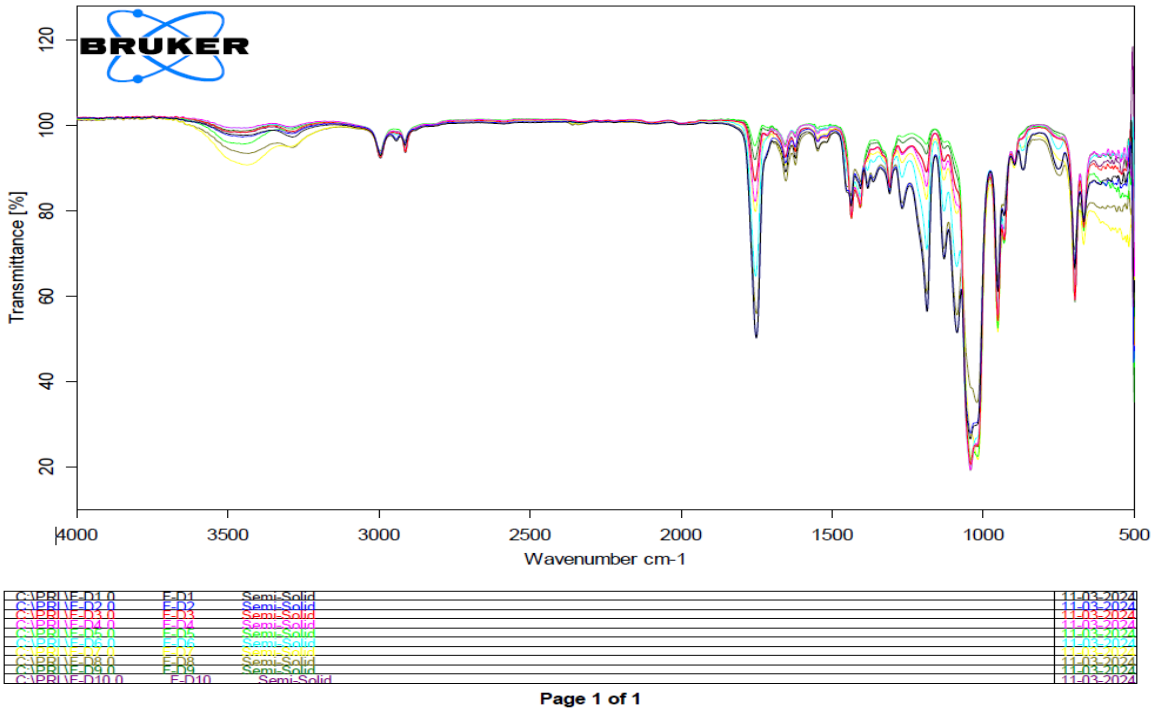

Figure 4: FTIR overlay Spectra of GA formulations

Differential Scanning Calorimetry

DSC was employed to evaluate the thermal behaviour and compatibility of GA with the PLGA polymer matrix. The thermograms demonstrated distinct endothermic transitions corresponding to the melting behaviour of crystalline GA and the glass transition of amorphous PLGA, as shown in **Figure 5**. Analysis of the physical mixture revealed modified thermal events, including shifts in transition temperatures and changes in enthalpy values, and maintained the characteristic thermal signatures of both components. The preserved thermal properties of both elements in the mixture further support the maintenance of their structural integrity and the formation of a physically stable composite matrix.

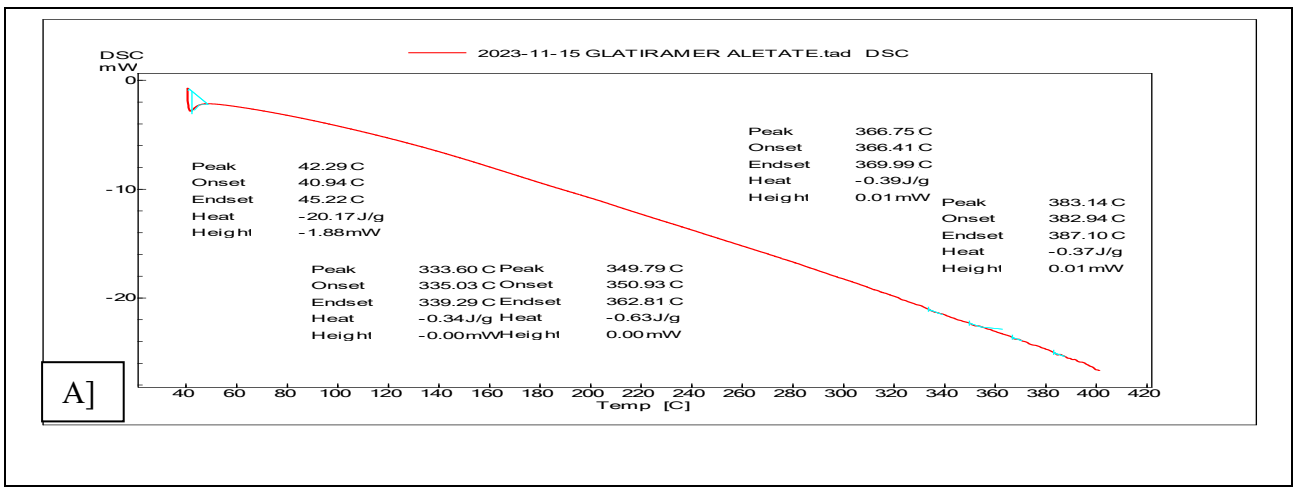

Journal of Chemical Health Risks

www.jchr.org

JCHR (2026) 16(1), 1402-1419 | ISSN:2251-6727

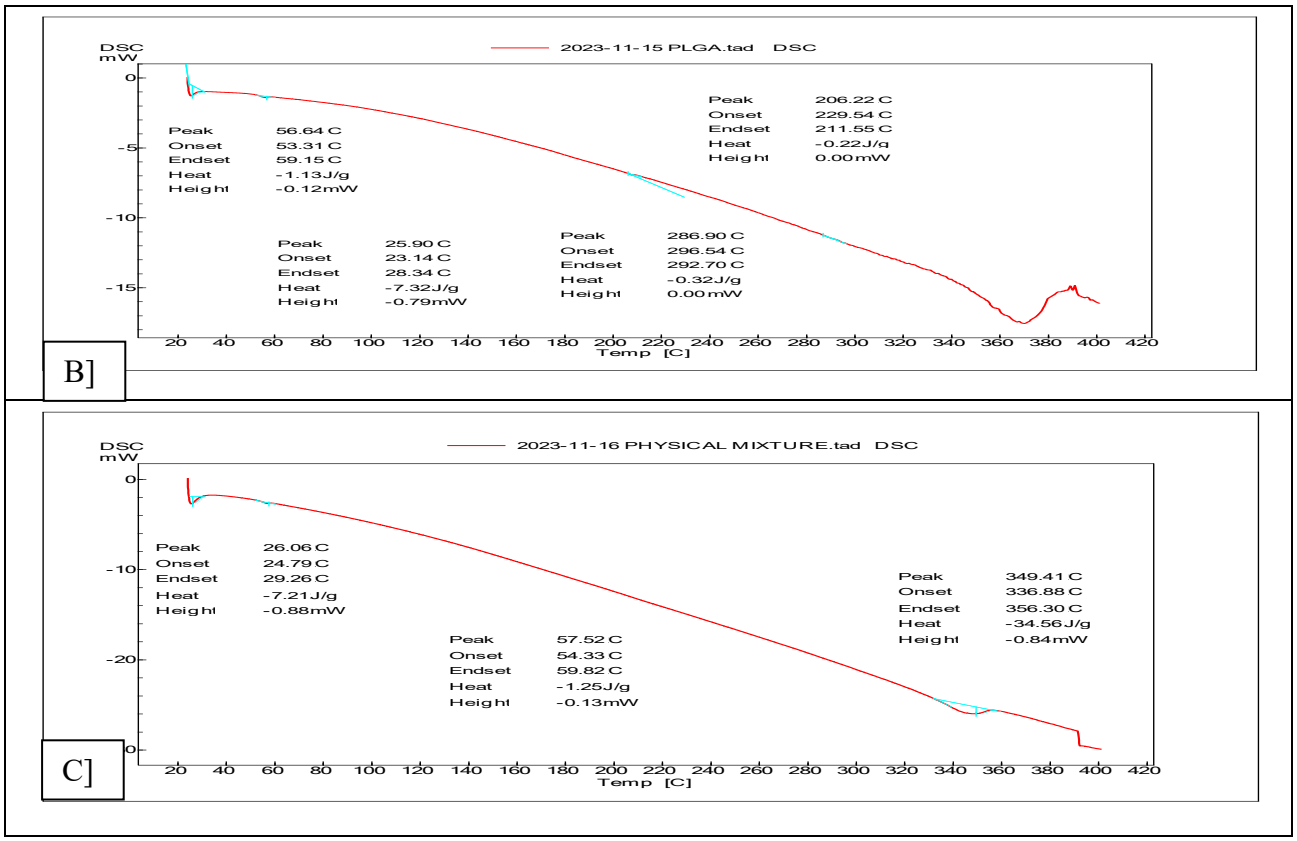

Figure 5: DSC Thermogram of A] GA; B] PLGA Polymer; C] Physical Mixture

X-ray Diffraction Pattern

The diffraction pattern of pure GA displayed distinct Bragg reflections at characteristic 2θ angles, confirming its crystalline nature, as shown in **Figure 6**. Conversely, the AG formulations exhibited significant attenuation of these crystalline peaks, along with the emergence of a broad halo. This remarkable reduction in crystallinity indicates successful molecular dispersion of GA within the polymer matrix, with the drug transitioning to an amorphous state, which is expected to enhance dissolution and controlled-release kinetics.

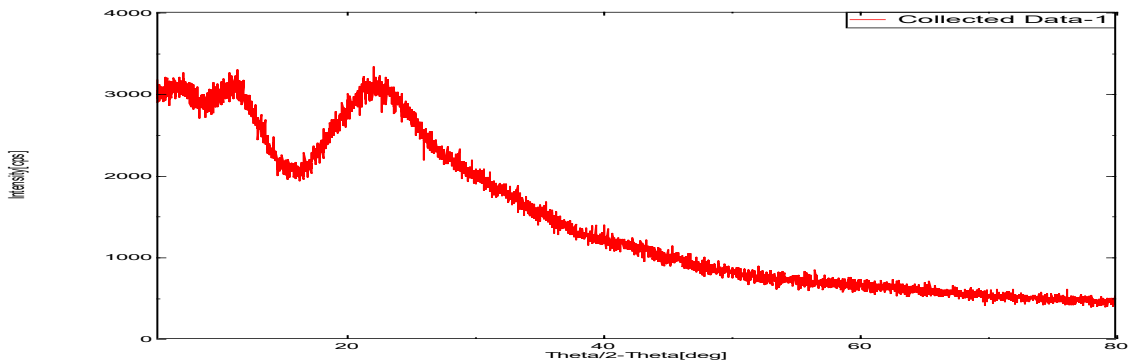

Journal of Chemical Health Risks

www.jchr.org

JCHR (2026) 16(1), 1402-1419 | ISSN:2251-6727

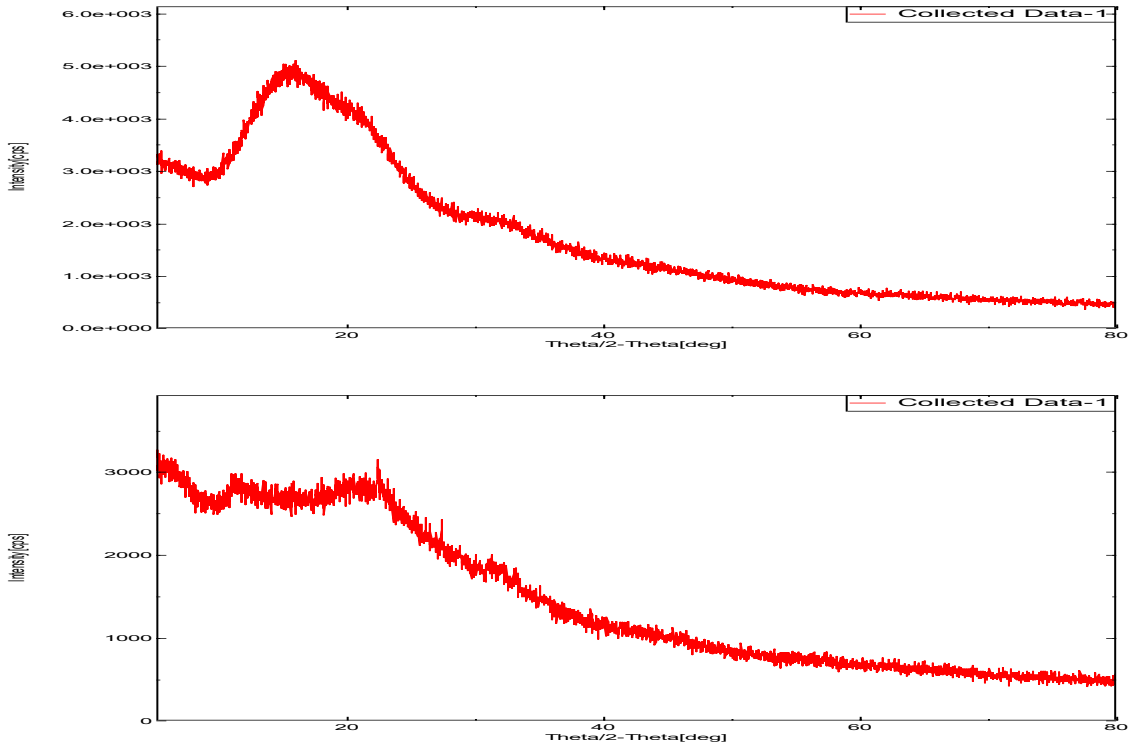

Figure 6: XRD Spectra of A] GA; B] AG Formulation; C] PLGA Polymer

Particle morphology

The microstructural analysis demonstrated three distinct morphological profiles, as shown in **Figure 7**. The GA has a crystalline structure, exhibiting angular facets and sharp edges. The polymer particles are irregular aggregates with a porous surface. Physically homogeneous mixtures exhibit intermediate characteristics. Notably, the GA-incorporated AG systems demonstrated consistently smooth matrices with submicron surface roughness (Ra < 100 nm), as quantified by image analysis software. GA's appearance is very soft, whereas the physical mixtures appear uniform in appearance, consisting of a homogeneous mixture of polymer and drug.

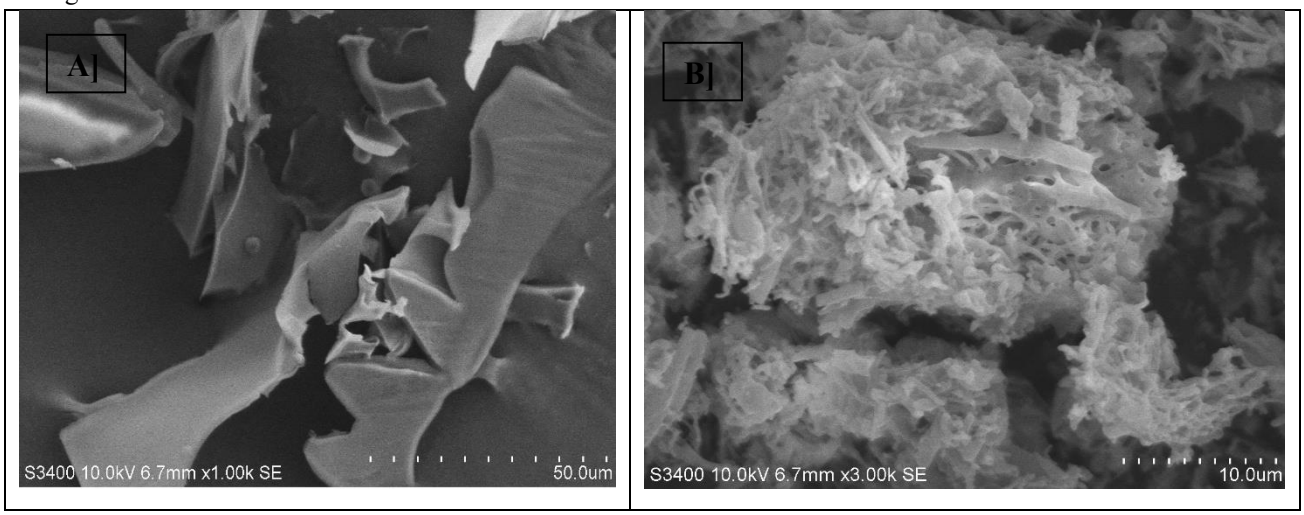

Journal of Chemical Health Risks

www.jchr.org

JCHR (2026) 16(1), 1402-1419 | ISSN:2251-6727

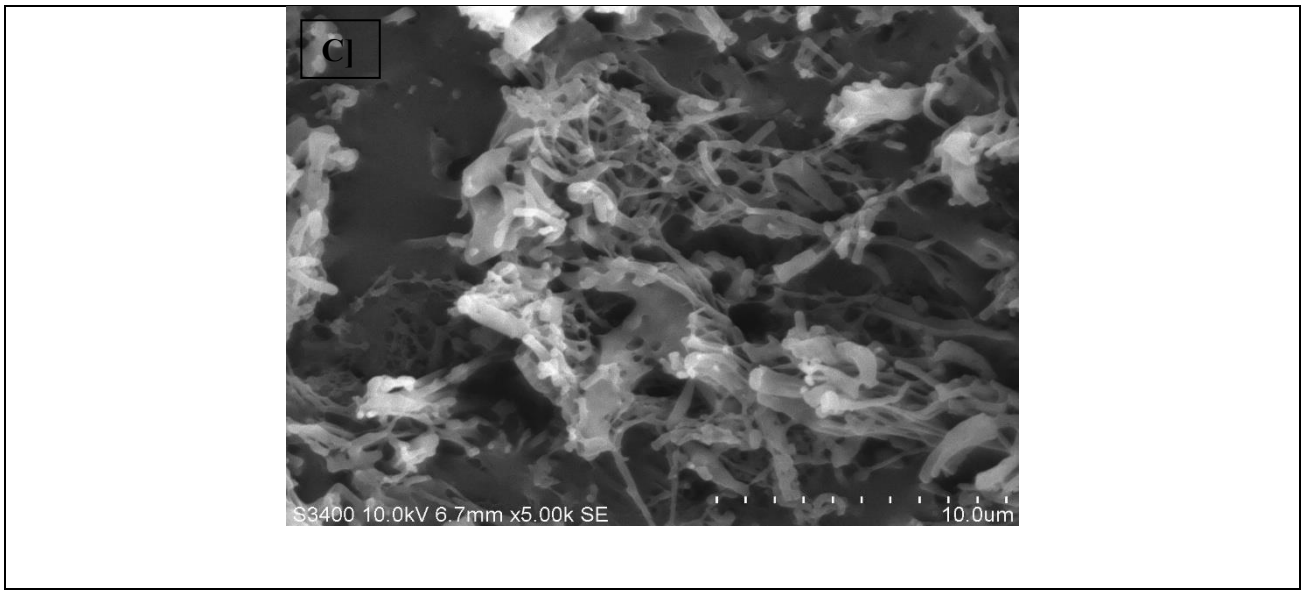

Figure 7: Morphology of A] GA; B] Physical Mixture; C] Polymer PLGA SEM Image.

In-vitro Dissolution

The dissolution profiles of GA, the drug-polymer mixture (Physical Mixture-PM), and the optimised formulation were studied in 7.4 phosphate buffer, and the results are graphically represented in Figure 8A. PM shows a slight decrease in the dissolution profile with increasing time relative to GA. The cumulative dissolution of PM was 100% in 75 hours, whereas that of GA was 20 hours. The in situ-forming GA implant showed 61.18% cumulative dissolution within 75 hours. In a pH phosphate buffer, the similarity factor f2 for the dissolution profiles of GA was 26, and f1 is likewise less than for GA implant and PM. In situ implant demonstrated significantly superior controlled release than GA and PM. The extended dissolution rate of the GA implant was therefore inferred to indicate good drug delivery, which will increase half-life and extend duration of action, thereby decreasing the dose frequency.

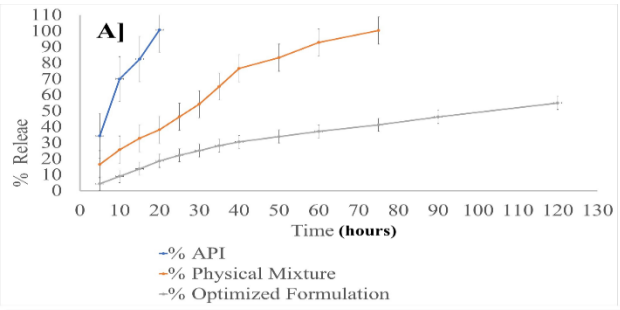

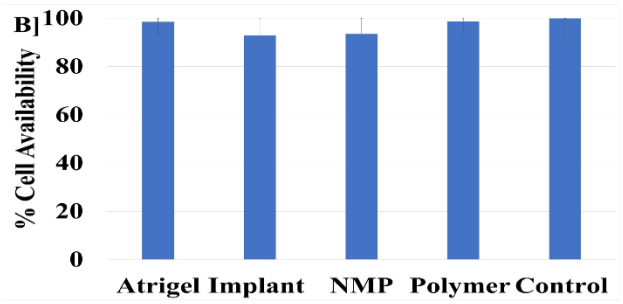

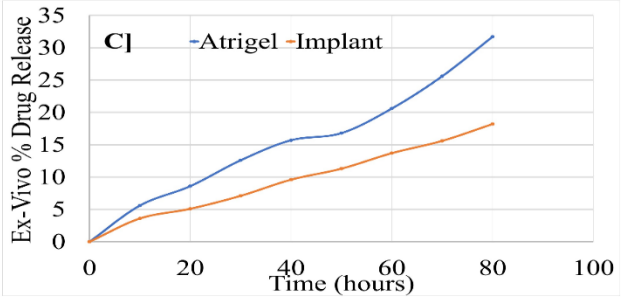

Figure 8: Results A] In vitro % Drug release; B] % Cell Availability; C] Ex vivo % Drug Release

Journal of Chemical Health Risks

www.jchr.org

JCHR (2026) 16(1), 1402-1419 | ISSN:2251-6727

Ex Vivo Evaluation of GA AG Samples

The ex vivo study was conducted to assess the formation and morphology of AGs and implants (PLGA 504H) and to evaluate the release kinetics of the active GA from hen drumstick tissue. To confirm depot formation, the injected formulations were examined 24 hours post-administration by dissecting the drumstick tissue, as illustrated in **8C**; the red frames highlight the subcutaneous deposition of the implant and gel, respectively. Ex vivo drug release was monitored over 72 hours, after which the release medium exhibited signs of degradation. Comparative analysis of release profiles from in situ-forming gels and in situ-forming implants revealed no statistically significant differences ($p > 0.05$) between ex vivo and in vitro release kinetics, confirming consistent behaviour upon subcutaneous administration.

In Vitro In Vivo Correlation (IVIVC)

The In Vitro In Vivo Correlation (IVIVC) for the AG formulation was established through a comparative analysis of in vitro dissolution and ex vivo release data. The in vitro dissolution study in pH 7.4 phosphate buffer revealed that the GA (GA) in situ forming implant exhibited a controlled release profile, with only 61.18% cumulative drug release over 75 hours, significantly slower than the physical mixture (PM) and pure GA, which released 100% within 75 hours and 20 hours, respectively. The similarity factors ($f2 = 26$, $f1 < 15$) further confirmed the distinct release kinetics of the implant, suggesting its potential for extended drug delivery. The ex vivo study in hen drumstick tissue demonstrated consistent subcutaneous depot formation, with no significant difference ($p > 0.05$) between in vitro and ex vivo release profiles over 72 hours, indicating reliable in vivo predictability. These findings suggest a strong correlation between in vitro dissolution and ex vivo release, supporting the AG formulation's ability to sustain drug release, prolong half-life, and reduce dosing frequency in vivo.

In Vitro Cytotoxicity Assessment of Formulations on L929 Fibroblasts

The adipose tissue-derived mouse L929 fibroblast cell line was selected for cytotoxicity testing due to its relevance to subcutaneous connective tissue. Fibroblasts are a prominent cell type in the dermal layer and serve as a suitable model for assessing biocompatibility. The mitochondrial dehydrogenase activity in viable cells was determined by measuring the reduction of MTT to formazan for cytotoxicity. The fibroblast viability after 24 hours of exposure to the formulations ranged 92.8~99.9%, confirming acceptable biocompatibility, as shown in **Figure 8 C]**. AG sample demonstrated significantly higher cell viability (98.5 ± 1.15%) compared to the implant (92.8 ± 2.93%) ($p < 0.008$), attributed to the reduced burst release of NMP over the initial 24 hours. The current research findings are consistent with in vitro release data, supporting the conclusion that the AG formulation is biocompatible and suitable for subcutaneous use.

DISCUSSION

The development of a long-acting AG formulation of GA for MS therapy represents a significant advancement in addressing treatment adherence challenges [31-33]. Our optimised formulation exhibits controlled-release kinetics, with only 61.18% cumulative drug release within 75 minutes, whereas bulk GA occurs within 20 minutes. This sustained-release profile could be attributed to optimisation of the drug-to-polymer ratio and solvent concentration, suggesting the potential to reduce dose frequency while maintaining therapeutic efficacy. The factorial design approach demonstrated a correlation between formulation variables and key performance attributes, with higher polymer ratios effectively modulating release rates. These findings align with previously established principles of PLGA-based depot systems, in which polymer composition and solvent selection significantly influence drug-release patterns [37-38]. Equation 2 for viscosity includes a negative coefficient for solvent concentration, which means that increasing solvent concentration typically lowers viscosity. This is mainly attributable to the solvent NMP. NMP is a strong solvent that reduces the apparent viscosity of the formulation by weakening intermolecular interactions within the polymer.

Comprehensive physicochemical characterisation confirmed the formulation's structural integrity and performance. SEM and XRD results demonstrated the transition of crystalline GA to an amorphous state within the PLGA matrix. DSC and FTIR results demonstrated chemical compatibility among the ingredients, with no chemical interactions. The developed UV spectroscopic method exhibited excellent linearity for the reliable

quantification of the drug. In this study, the effects of the drug-to-polymer ratio and solvent concentration were investigated. It was found that the AG system has a significant impact on drug release compared to the simple injection of GA. A polymer exhibiting good stability in NMP is found to have better physical properties in formulation than in other solvents.

Biological evaluations also demonstrated AG's potential; an ex vivo drumstick model study showed a release profile comparable to in vitro results, thereby validating the formation of a depot. Cytotoxicity assessments using L929 fibroblasts revealed excellent biocompatibility (97.8-100% viability), particularly for the AG formulation (98.5 ± 1.15%), consistent with previous reports on similar delivery systems [27, 28, 40]. Prior studies by Rahimi et al. demonstrated that in situ formulation implant systems exhibit fibroblast viability in the range of 96~100%, indicating minimal cytotoxicity [41].

The clinical application of the current research is substantial, offering a potential solution to patient compliance challenges associated with daily GA injections. The sustained release characteristics may enable less frequent dosing while maintaining therapeutic drug levels, similar to advanced long-acting injectables. The amorphous nature of GA in the AG formulation will enhance solubility and bioavailability, potentially enabling dose reduction. However, more evidence is needed to claim the higher bioavailability and dose reduction. The AG platform technology is suitable not only for GA delivery but also for other MS therapeutics requiring sustained-release profiles.

CONCLUSION

This study demonstrated the development and optimisation of a GA AG drug delivery system for the management of multiple sclerosis. Using a systematic approach with a 32-run randomised complete factorial design, the impact of key formulation parameters, such as drug-to-polymer ratio and solvent concentration, was evaluated. The AG system exhibited superior performance in drug encapsulation, stability, and controlled release compared with traditional formulations. Comprehensive characterisation using SEM, UV spectroscopy, DSC, XRD, and FTIR confirmed the physical and chemical integrity of the formulation. In vitro dissolution studies demonstrated extended drug-release profiles, which are expected to enhance therapeutic efficacy while reducing dosing frequency, as shown in ex vivo and in vivo studies. These results highlight the potential of the AG system as a promising alternative to conventional daily injections, offering improved patient compliance and extended action.

Acknowledgement

The author expresses their sincere gratitude to Dr Rajesh Khathuriya, Ms Vrushali A. Kulkarni, and Pacific Academy of Higher Education and Research University, Udaipur, Rajasthan, India, for their support and for providing the facilities for this research. Lastly, we are grateful to all colleagues and collaborators who have provided valuable suggestions and assistance throughout the study.

Conflict of Interest

The authors declare no conflicts of interest related to this study or its publication.

References

1. Compston A, Coles A. Multiple sclerosis. The Lancet [Internet]. 2002 Apr 1;359(9313):1221–1231. Available from: https://pubmed.ncbi.nlm.nih.gov/11955556/
2. Noseworthy JH, Lucchinetti C, Rodriguez M, Weinshenker BG. Multiple sclerosis. New England Journal of Medicine [Internet]. 2000 Sep 28;343(13):938–952. Available from: https://pubmed.ncbi.nlm.nih.gov/11006371/
3. Ruggieri M, Avolio C, Livrea P, Trojano M. GA in multiple sclerosis: a review. CNS Drug Reviews [Internet]. 2007 Jun 1;13(2):178–191. Available from: https://pubmed.ncbi.nlm.nih.gov/17627671/
4. Goldenberg M. Multiple sclerosis review. Pharmacy and therapeutics, 2012 Mar;37(3):175–184. Available from: https://pmc.ncbi.nlm.nih.gov/articles/PMC3351877/pdf/ptj3703175.pdf.
5. Ghasemi N, Razavi S, Nikzad E. Multiple Sclerosis: Pathogenesis, Symptoms, Diagnoses and Cell-Based Therapy. DOAJ (DOAJ:

Directory of Open Access Journals) [Internet]. 19(1):1–10. Available from: https://doaj.org/article/5633ef82a00b4c57a2b148297ae81aa3

6. Ziemssen T. Modulating processes within the central nervous system is central to therapeutic control of multiple sclerosis. Journal of Neurology [Internet]. 2005 Oct 1;252(S5):v38–v45. Available from: https://pubmed.ncbi.nlm.nih.gov/16254701/

7. Goldberg L, Edwards NC, Fincher C, Doan QV, Al-Sabbagh A, Meletiche DM. Comparing the Cost-Effectiveness of Disease-Modifying Drugs for the First-Line treatment of Relapsing-Remitting Multiple sclerosis. Journal of Managed Care Pharmacy [Internet]. 2009 Sep 1;15(7):543–555. Available from: https://pubmed.ncbi.nlm.nih.gov/19739877/

8. Dobson R, Giovannoni G. Multiple sclerosis – a review. European Journal of Neurology [Internet]. 2018 Oct 10;26(1):27–40. Available from: https://pubmed.ncbi.nlm.nih.gov/30300457/

9. Filippi M, Bar-Or A, Piehl F, Preziosa P, Solari A, Vukusic S, Rocca MA. Multiple sclerosis. Nature Reviews Disease Primers [Internet]. 2018 Nov 8;4(1). Available from: https://pubmed.ncbi.nlm.nih.gov/30410033/

10. Rodriguez M. Diagnosis and management of multiple sclerosis. Journal of Neuropathology & Experimental Neurology [Internet]. 2003 May 1;62(5):590. Available from: https://doi.org/10.1093/jnen/62.5.590

11. Hahn JS, Pohl D, Rensel M, Rao S. Differential diagnosis and evaluation in pediatric multiple sclerosis. Neurology [Internet]. 2007 Apr 16;68(16_suppl_2). Available from: https://doi.org/10.1212/01.wnl.0000259403.31527.ef

12. Gelfand JM. Multiple sclerosis. Handbook of Clinical Neurology [Internet]. 2014 Jan 1;269–290. Available from: https://pubmed.ncbi.nlm.nih.gov/24507522/

13. Ciotti JR, Cross AH. Disease-Modifying treatment in progressive multiple sclerosis. Current Treatment Options in Neurology [Internet]. 2018 Apr 7;20(5). Available from: https://doi.org/10.1007/s11940-018-0496-3

14. Oh J, Bar-Or A. Emerging therapies to target CNS pathophysiology in multiple sclerosis. Nature Reviews Neurology [Internet]. 2022 Jun 13;18(8):466–475. Available from: https://doi.org/10.1038/s41582-022-00675-0

15. Gholamzad M, Ebtekar M, Ardestani MS, Azimi M, Mahmodi Z, Mousavi MJ, Aslani S. A comprehensive review on the treatment approaches of multiple sclerosis: currently and in the future. Inflammation Research [Internet]. 2018 Sep 3;68(1):25–38. Available from: https://pubmed.ncbi.nlm.nih.gov/30178100/

16. Rocco P, Eberini I, Musazzi UM, Franzè S, Minghetti P. GA: A complex drug beyond biologics. European Journal of Pharmaceutical Sciences [Internet]. 2019 Mar 19;133:8–14. Available from: https://doi.org/10.1016/j.ejps.2019.03.011

17. Lalive PH, Neuhaus O, Benkhoucha M, Burger D, Hohlfeld R, Zamvil SS, Weber MS. GA in the treatment of multiple sclerosis. CNS Drugs [Internet]. 2011 Mar 30;25(5):401–414. Available from: https://pmc.ncbi.nlm.nih.gov/articles/PMC3963480/

18. Label FDA. COPAXONE (GA injection), for subcutaneous use. Teva Neuroscience, Inc, Parsippany, NJ 07054 [Internet]. 2024;119(13):1–29. Available from: https://www.accessdata.fda.gov/drugsatfda_docs/label/2025/020622s118s119lbl.pdf

19. Varkony H, Weinstein V, Klinger E, Sterling J, Cooperman H, Komlosh T, Ladkani D, Schwartz R. The glatiramoid class of immunomodulator drugs. Expert Opinion on Pharmacotherapy [Internet]. 2009 Feb 26;10(4):657–668. Available from: https://doi.org/10.1517/14656560902802877

20. Schrempf W, Ziemssen T. GA: Mechanisms of action in multiple sclerosis. Autoimmunity Reviews [Internet]. 2007 Mar 8;6(7):469–475. Available from: https://pubmed.ncbi.nlm.nih.gov/17643935/

21. Aharoni R, Milo R, Arnon R. GA for the treatment of multiple sclerosis: from first generation therapy to elucidation of immunomodulation and repair. Pharmacological Reviews [Internet]. 2024 Oct 15;76(6):1133–1158. Available from: https://pubmed.ncbi.nlm.nih.gov/39406508/

22. Mirabella M, Annovazzi P, Brownlee W, Cohen JA, Kleinschnitz C, Wolf C. Treatment challenges in multiple sclerosis – a continued role for GA? Frontiers in Neurology [Internet]. 2022 Apr 15;13. Available from: https://pubmed.ncbi.nlm.nih.gov/35493825/

23. Denis L, Namey M, Costello K, Frenette J, Gagnon N, Harris C, Lowden D, McEwan L, Morrison W, Poirier J. Long-Term Treatment Optimization in Individuals with Multiple Sclerosis Using Disease-Modifying Therapies. Journal of Neuroscience Nursing [Internet]. 2004 Feb 1;36(1):10–22. Available from: https://pubmed.ncbi.nlm.nih.gov/14998102/

24. Flechter S, Popper L, Demender I, Kimelman NB, Rubnov S, Danon U, Marom E, Milo R, Gilad R, Weller B, Vaknin-Dembinsky A, Hellmann M, Karni A. GA Depot (extended-release) phase IIa study in patients with Primary Progressive Multiple Sclerosis: safety and efficacy snapshot (1911). Neurology [Internet]. 96(15_supplement). Available from: https://doi.org/10.1212/wnl.96.15_supplement.1911

25. Thakur RRS, McMillan HL, Jones DS. Solvent induced phase inversion-based in situ forming controlled release drug delivery implants. Journal of Controlled Release [Internet]. 2014 Jan 2;176:8–23. Available from: https://pubmed.ncbi.nlm.nih.gov/24374003/

26. Park K, Otte A, Sharifi F, Garner J, Skidmore S, Park H, Jhon YK, Qin B, Wang Y. Formulation composition, manufacturing process, and characterization of poly(lactide-co-glycolide) microparticles. Journal of Controlled Release [Internet]. 2020 Oct 24;329:1150–1161. Available from: https://pmc.ncbi.nlm.nih.gov/articles/PMC7904638/

27. Kamali H, Khodaverdi E, Hadizadeh F, Mohajeri SA. In-vitro, ex-vivo, and in-vivo evaluation of buprenorphine HCl release from an in situ forming gel of PLGA-PEG-PLGA using N-methyl-2-pyrrolidone as solvent. Materials Science and Engineering C [Internet]. 2018 Nov 28;96:561–575. Available from: https://doi.org/10.1016/j.msec.2018.11.058

28. Avachat AM, Kapure SS. Asenapine maleate in situ forming biodegradable implant: An approach to enhance bioavailability. International Journal of Pharmaceutics [Internet]. 2014 Oct 9;477(1–2):64–72. Available from: https://doi.org/10.1016/j.ijpharm.2014.10.006

29. Torabi S, Soleimani S, Mahravani H, Ebrahimi MM, Shahsavandi S. Mouse fibroblast L929 cell line as a useful tool for replication and adaptation of infectious bursal disease virus. PubMed [Internet]. 2023 Jun 1;78(3):863–871. Available from: https://pubmed.ncbi.nlm.nih.gov/38028862

30. Liu Q, Zhang H, Zhou G, Xie S, Zou H, Yu Y, Li G, Sun D, Zhang G, Lu Y, Zhong Y. In vitro and in vivo study of thymosin alpha1 biodegradable in situ forming poly(lactide-co-glycolide) implants. International Journal of Pharmaceutics [Internet]. 2010 Jul 21;397(1–2):122–129. Available from: https://doi.org/10.1016/j.ijpharm.2010.07.015

31. Wang X, Burgess DJ. Drug release from in situ forming implants and advances in release testing. Advanced Drug Delivery Reviews [Internet]. 2021 Aug 5;178:113912. Available from: https://doi.org/10.1016/j.addr.2021.113912

32. Mahakul S, Srivastava P, Tiwari S. AG Technology: A Biodegradable Repository for Long-Term Drug Release. Tanz Journal,

2025;20(5):413-424. https://tanzj.net/wp-content/uploads/2025/05/35-TJ1961.pdf

33. Dunn R. The AG drug delivery system. CRC Press eBooks [Internet]. 2002. p. 671–680. Available from: https://doi.org/10.1201/9780203910337-57

34. Shobeirean A, Attar H, Varshochian R, Rezvanfar M. GA in situ forming gel, a new approach for multiple sclerosis treatment. DARU Journal of Pharmaceutical Sciences, 2024;32:649–664. Available from: https://doi.org/10.1007/s40199-024-00532-z

35. Lakshmi V. Formulation and evaluation of polyherbal cream. Int. J. Pharm. Pharm. Sci., 2025; 7(2): 36-42. Available From: https://doi.org/10.33545/26647222.2025.v7.i2a.191

36. Shinghai M, Kori M. Formulation and evaluation of invasomal gel of adapalene for effective acne treatment. Asian Journal of Pharmaceutical and Clinical Research, 2025;18(8):183-188.

37. Saha S, Lin X, Zhou L, Xue A, Gosselin E, Chothe PP, Darji M, Lu X, Yang W. Evaluation of the impact of the polymer end groups and molecular weight on in vitro and in vivo performances of PLGA based in situ forming implants for ketoprofen. Journal of Pharmaceutical Sciences [Internet]. 2024 Oct 1; Available from: https://doi.org/10.1016/j.xphs.2024.10.019

38. Hu F, Qi J, Lu Y, He H, Wu W. PLGA-based implants for sustained delivery of peptides/proteins: Current status, challenge and perspectives. Chinese Chemical Letters [Internet]. 2023 Feb 24;34(11):108250. Available from: https://doi.org/10.1016/j.cclet.2023.108250

39. Southard G, Dunn R, Garrett S. The drug delivery and biomaterial attributes of the AGtechnology in the treatment of periodontal disease. Expert Opinion on Investigational Drugs [Internet]. 1998 Sep 1;7(9):1483–1491. Available from: https://doi.org/10.1517/13543784.7.9.1483

40. Ravivarapu HB, Moyer KL, Dunn RL. Sustained suppression of pituitary-gonadal axis with an injectable, in situ forming implant of leuprolide acetate. Journal of Pharmaceutical Sciences [Internet]. 89(6):732–741. Available from: https://doi.org/10.1002/(SICI)1520-6017(200006)89:6%3C732::AID-JPS4%3E3.0.CO;2-D

41. Cannella V, Altomare R, Leonardi V, Russotto L, Di Bella S, Mira F, Guercio A. In vitro biocompatibility evaluation of nine dermal fillers on L929 cell line. BioMed Research International [Internet]. 2020 May 27;2020:1–6. Available from: https://doi.org/10.1155/2020/8676343